JIPB Journal of Integrative Plant Biology

Plastid ribosomal protein LPE2 is involved in photosynthesis and the response to C/N balance in *Arabidopsis thaliana*[OO]

Xiaoxiao Dong[1†], Sujuan Duan[1,2†], Hong-Bin Wang[1] and Hong-Lei Jin[2]*

1. School of Life Sciences, Sun Yat-sen University, Guangzhou 510275, China
2. School of Pharmaceutical Sciences, Guangzhou University of Chinese Medicine, Guangzhou 510006, China
†These authors contributed equally to this work.
*Correspondence: Hong-Lei Jin (jinhl@gzucm.edu.cn)
doi: 10.1111/jipb.12907

Abstract The balance between cellular carbon (C) and nitrogen (N) must be tightly coordinated to sustain optimal growth and development in plants. In chloroplasts, photosynthesis converts inorganic C to organic C, which is important for maintenance of C content in plant cells. However, little is known about the role of chloroplasts in C/N balance. Here, we identified a nuclear-encoded protein LOW PHOTOSYNTHETIC EFFICIENCY2 (LPE2) that it is required for photosynthesis and C/N balance in *Arabidopsis*. LPE2 is specifically localized in the chloroplast. Both loss-of-function mutants, *lpe2-1* and *lpe2-2*, showed lower photosynthetic activity, characterized by slower electron transport and lower PSII quantum yield than the wild type. Notably, *LPE2* is predicted to encode the plastid ribosomal protein S21 (RPS21). Deficiency of LPE2 significantly perturbed the thylakoid membrane composition and plastid protein accumulation, although the transcription of plastid genes is not affected obviously. More interestingly, transcriptome analysis indicated that the loss of LPE2 altered the expression of C and N response related genes in nucleus, which is confirmed by quantitative real-time-polymerase chain reaction. Moreover, deficiency of LPE2 suppressed the response of C/N balance in physiological level. Taken together, our findings suggest that LPE2 plays dual roles in photosynthesis and the response to C/N balance.

Edited by: Martin A.J. Parry, Lancaster University, UK
Received Dec. 1, 2019; **Accepted** Jan. 9, 2020; **Online on** Jan. 15, 2020
OO: OnlineOpen

Research Article

OnlineOpen

INTRODUCTION

Chloroplasts have evolved in eukaryotic cells through the process of endosymbiosis. Although most genes from chloroplast were transferred to the nucleus during endosymbiosis, approximately 80 chloroplast proteins are encoded by the chloroplast genome (Timmis et al. 2004). This implies that plastids have retained the machinery required for basic genetic processes including DNA replication, RNA transcription, and protein translation. Translation in plastids is mediated by the 70S ribosome, which comprises a small 30S subunit and a large 50S subunit. The small and large subunits of 70S ribosome function in reading the transcript and synthesizing polypeptides, respectively. Both subunits of 70S ribosome contain different ribosomal RNAs (rRNAs) and plastid ribosomal proteins (RPs) (Yamaguchi and Subramanian 2000; Tiller et al. 2012). Plastid RPs play multiple roles in plant growth and development (Romani et al. 2012). Most of the RPs are indispensable for the development of chloroplasts, such as *prpl1*, *prpl27*, *prps20*, *prpl28*, *prpl21*, *prpl35*, and *prpl4*, and the lack of these RPs causes embryo lethality (Rogalski et al. 2006,2008; Bryant et al. 2011; Tiller et al. 2012; Tiller and Bock 2014). By contrast, RPs such as *rps21*, *prpl11*, *prps1*, *prps17*, and *prpl24* are nonessential, and mutations

in these proteins do not affect plant survival (Pesaresi et al. 2001; Morita-Yamamuro et al. 2004; Tiller and Bock 2014). Nonetheless, the absence of these RPs causes several phenotypic changes. For example, RPL21c has an important function in chloroplast development in *Oryza sativa* L., and *rpl21c* mutants exhibit an albino and seed lethal phenotype (Lin et al. 2015). In *Arabidopsis thaliana*, the lack of PRPL11 and PRPS5 causes a pale green phonotype and growth rate and photosynthesis decreases sharply (Pesaresi et al. 2001; Zhang et al. 2016). The absence of PRPL4, PRPS20, PRPL27, PRPL1, or PRPL35 changes the pattern of cell division and perturbs embryo development in *Arabidopsis thaliana* (Romani et al. 2012). However, the specific regulatory mechanism of some RPs needs further investigation.

Chloroplasts not only host important metabolic processes, including fatty acid and amino acid biosynthesis, photosynthesis, and carotenoid metabolism (Leon et al. 1998; Neuhaus and Emes 2000), but also function as a sensor for detecting changes within and outside the chloroplast, ultimately generating a signal that regulates gene expression (Leon et al. 1998; Pogson and Albrecht 2011; Chan et al. 2016). Because the genome is divided between the chloroplast and nucleus, plants need a precise coordination between chloroplast and nuclear genomes to control plastid development. Plastids regulate nuclear gene expression by transmitting information about the state of plastid development and function to the nucleus, which is called retrograde signaling (Leon et al. 1998; Pogson and Albrecht 2011; Chan et al. 2016). Several major pathways of retrograde signaling have been described, depending on the source of the signal: (i) plastid gene expression (PGE); (ii) the activity of the photosynthetic electron transport (PET) chain; (iii) reactive oxygen species (ROS); (iv) tetrapyrrole biosynthesis pathway (TBP); and (v) plastid metabolism, such as SAL1–3′-phosphoadenosine5′-phosphate (PAP) and methylerythritol cyclodiphosphate (MEcPP) (Nott et al. 2006; Pesaresi et al. 2007; Pogson et al. 2008; Kleine et al. 2009; Estavillo et al. 2011; Xiao et al. 2012). The absence of PGE decreases the expression of photosynthesis-associated nuclear genes (PhANGs) (Sullivan and Gray 1999), as shown by the *Arabidopsis prolyl-tRNA synthetase 1* (*prors1*) mutant, which shows reduced synthesis of protein in the chloroplast (Pesaresi et al. 2006).

Retrograde signaling affects the life cycle of plants (Hernandez-Verdeja and Strand 2018). PGE-triggered retrograde signaling leads to embryo lethal phenotypes (Garcia et al. 2008; Hsu et al. 2010; Babiychuk et al. 2011). Retrograde signals have important functions in leaf lamina and mesophyll cells' development; this is supported by altered leaf shape and pigmentation in plants lacking ANU7 (Munoz-Nortes et al. 2017). Additionally, retrograde signaling plays an important role in cell expansion and photosynthesis activation via tetrapyrroles (Andriankaja et al. 2012). It is reported that flowering time can also be regulated by retrograde signaling (Baba et al. 2004; Albrecht et al. 2006; Feng et al. 2016). However, more processes involving retrograde signaling need to be demonstrated experimentally.

Here, we identified two loss-of-function mutants of the *Arabidopsis LOW PHOTOSYNTHETIC EFFICIENCY2* (*LPE2*) gene (At3g27160) using a chlorophyll fluorescence video imaging system, which indicates the state of the PET chain. The disruption of *LPE2* resulted in reduced photosynthetic activity. LPE2 is located in chloroplast and is predicted to be a plastid RP. We show that deficiency of LPE2 significantly perturbed the accumulation of plastid protein. Moreover, our transcriptome data indicated that the lack of LPE2 altered the expression of genes related to response to carbon (C)/nitrogen (N) balance. Physiological experiments showed that the deficiency of *LPE2* suppressed the response to C/N balance, suggesting that the putative plastid translation signal mediated by LPE2 regulates response to C/N balance probably via retrograde signaling.

RESULTS

Photosynthetic capacity is reduced in *lpe2* mutants

To elucidate the mechanism of photosynthesis regulation, we screened several *Arabidopsis* mutants using chlorophyll fluorescence imaging (Meurer et al. 1996), and identified mutants with low photosynthetic efficiency (Jin et al. 2018). Consequently, we identified a T-DNA insertion mutant *lpe2* (*At3g27160*, SALK_077692); the photosystem II (PSII) maximum photosynthetic efficiency (F_v/F_m) in this mutant was drastically reduced compared to that of wild-type (WT) plants (Figure 1A–D). We named this mutant as *lpe2-1*. We also obtained another homozygous T-DNA insertion mutant of *LPE2* (CS843433) from *Arabidopsis* Biological Resource Center (ABRC) (Figure 1A), which were named as *lpe2-2*. In both lines of

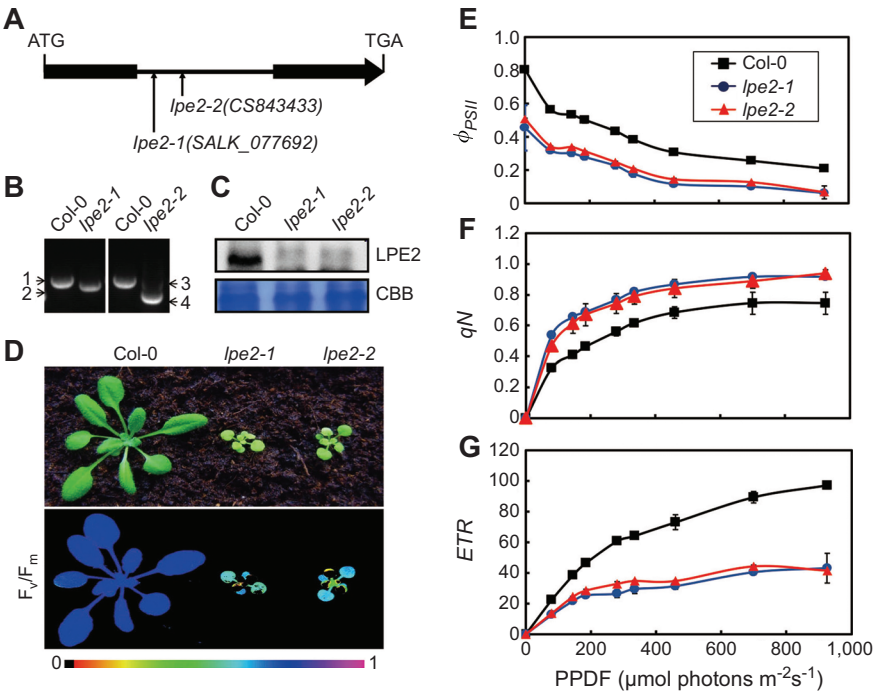

Figure 1. Mutations of the *LOW PHOTOSYNTHETIC EFFICIENCY2 (LPE2)* gene cause altered chlorophyll fluorescence parameters

(**A**) Schematic diagram of *LPE2* gene (At3g27160) inferred by DNA sequence analysis. Exons (black boxes) and introns (lines) are indicated. The positions of the T-DNA insertions corresponding to *lpe2-1* and *lpe2-2* are shown. ATG start codon and TGA stop coden are shown. (**B**) Polymerase chain reaction (PCR) analysis of genomic DNA from the wild type and *lpe2* mutants to confirm the homozygosity of the mutants. 1 and 2, amplification with primers F and R for SALK_077692 and Lba1; 3 and 4, amplification with primers F and R for CS843433 and Lba1. (**C**) Relative level of LPE2 protein in wild-type (WT) and *lpe2* mutant plants. CBB, Coomassie blue staining. (**D**) Imagines in (a) are of 3-week-old wild type (Col-0), *lpe2-1*,and *lpe2-2* plants under growth light conditions. (b) False-color images representing F_v/F_m under a growth light condition in 3-week-old wild-type, *lpe2-1*, and *lpe2-2* plants. The false color ranged from black (0) via red, orange, yellow, green, blue, and violet to purple (1) as indicated at the bottom. Growth light (−100 μmol photons m^2/s). Six biological replicates were performed in all experiments, and similar results were obtained. (**E, F**), Light-response curves of PSII quantum yield (ΦPSII) (**E**), non-photochemical quenching(qN) (**F**), and electron transport rate (ETR) (**G**) in the wild type and *lpe2* mutants. Measurements were performed at the following light intensities: 0, 81,145, 186, 281, 335, 461, 701, and 926 mmol photons m^2/s^{-1}. PPDF, Photosynthetic photon flux density. Each data point represents at least 20 independent plants.

mutants, the T-DNA was inserted into the intron of the *LPE2* gene (Figure 1A). The homozygosity of both lines of mutants were analyzed by polymerase chain reaction (PCR) with three primers (Figure 1B). Protein detection showed that the expression of LPE2 protein was disturbed in both lines of mutants (Figure 1C). Both homozygotes showed light green leaves and dwarf plants (Figure 1D).

Next, to further precisely analyze the photosynthetic light reaction activity of mutants, we detected the light response curves of PSII quantum yield (Φ_{PSII}), non-photochemical quenching (qN), and electron transport rate (ETR). Compared with the WT, Φ_{PSII} (Figure 1E) and ETR (Figure 1G) were much lower in *lpe2* mutants, whereas qN was much higher in both mutants (Figure 1F). These data, combined with lower F_v/F_m in *lpe2* mutant plants (Figure 1D), confirm that the photosynthetic light reaction activity of mutants impaired in *lpe2* mutants. Therefore, the mutants SALK_077692 and CS843433 are hereafter referred to as *lpe2-1* and *lpe2-2*, respectively.

LOW PHOTOSYNTHETIC EFFICIENCY2 (LPE2) protein is specifically localized in chloroplasts

To detect the role of LPE2 in photosynthesis regulation, we first determined the subcellular localization

of LPE2. It is predicted that the *LPE2* gene encodes a 183 amino acid plastid RP named S21 (At3g27160) (Romani et al. 2012), according to the annotation of The *Arabidopsis* Information Resource (TAIR). Based on TargetP prediction, LPE2 contains a chloroplast transit peptide in N-terminal of protein (1–47 aa) (Emanuelsson et al. 2000) (Figure 2A). To determine whether LPE2 is localized in the chloroplast, a fused construct of the green fluorescent protein (GFP) with LPE2 under the control of the *35S* promoter (35S:LPE2-GFP) was expressed transiently in protoplasts of *Arabidopsis*. Confocal laser scanning of LPE2-GFP fusion protein revealed that LPE2 is located in the chloroplast specifically (Figure 2B). To determine the precise sub-location of LPE2, we further extracted chloroplasts from WT plants, and separated the stroma and thylakoid membrane fractions. Immunoblot analyses of the membrane and soluble fractions of chloroplasts indicated that LPE2 was mainly found in the stroma, besides a small amount in the thylakoid membrane (Figure 2C).

Thylakoid composition and plastid protein accumulation are perturbed in *lpe2* plants

To check the effect of the absence of plastid RP on photosynthesis related protein in *lpe2* mutants, we first performed blue native-polyacrylamide gel electrophoresis (BN-PAGE) and analyzed the accumulation of photosystem complexes (Figure 3A). The abundance of PSII, PSI, Cytb6/f, and ATPase complex was approximately 70%, 24%, 17%, and 35% lower in *lpe2* mutants, respectively, than in WT plants, on an equal chlorophyll basis. The abundance of LHCII trimmer showed no difference and is used as a control (Figure 3A, B). To determine whether defects in accumulation of photosystem complexes were related to alterations in accumulation level of plastid proteins, we further analyzed the accumulation of specific subunits of the photosynthetic thylakoid membrane protein complexes by sodium dodecyl sulphate-polyacrylamide gel electrophoresis (SDS-PAGE) (Figure 3C). The abundance of PSII core subunits PsbA, PsbB, PsbC, and PsbD encoded by plastid genes were obviously decreased in *lpe2* thylakoids; levels of these proteins in *lpe2* mutants were 45%, 56%, 63%, and 71% lower than those in the WT plants, respectively (Figure 3D). The level of other photosystem subunits encoded by plastid genes, including PSI subunits (PsaB/C), ATPase β-subunit (ATPB), and Cytb6/f (Cytf), also showed a marked decline in mutant plants (Figure 3C). Interestingly, the level of PSI subunits PsaD encoded by nuclear genes is also decreased, suggesting that *lpe2* mutation destabilized the entire PSI complex (Figure 3C). Other nuclear-encoded thylakoid proteins, including the major PSII antenna protein Lhcb1 and the PSI antenna protein Lhca1, behaved like PSII and PSI, respectively (Figure 3C).

To check whether the decreased accumulation of photosynthesis-related protein was due to defects

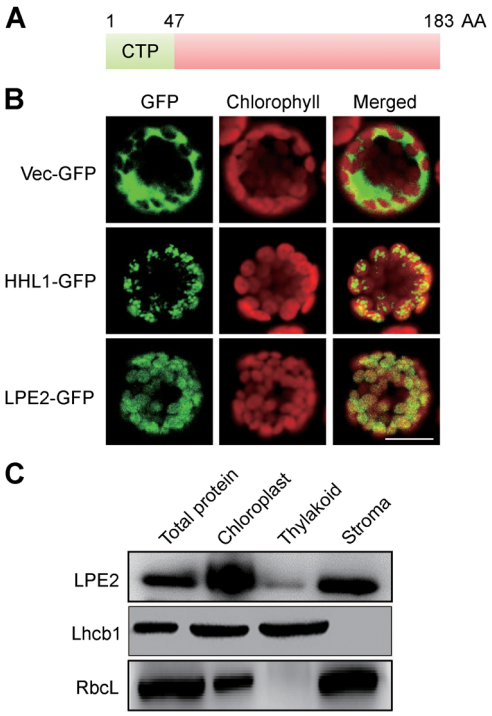

Figure 2. Subcellular localization of LOW PHOTOSYNTHETIC EFFICIENCY2 (LPE2) protein

(**A**) Schematic diagram of the LPE2 protein including chloroplast transit peptide (CTP). (**B**) Localization of LPE2 protein within the chloroplast by green fluorescent protein (GFP) assay in *Arabidopsis* protoplast. The fluorescence of LPE2-GFP specifically matched with that of chlorophyll autofluorescence, confirming chloroplast targeting of LPE2 exclusively. LPE2-GFP, LPE2-GFP fusion; Vec-GFP, control with empty vector; HHL1-GFP, HHL1-GFP fusion. Bars = 10 μm. (**C**) Immunolocalization of LPE2. Intact chloroplasts were isolated from leaves wild type plants and then separated into thylakoid membrane and stromal fractions. Polyclonal antibodies were used against the integral membrane protein, Lhcb1; the abundant stroma protein, ribulose bisphosphate carboxylase large subunit (RbcL); and LPE2. Three additional independent biological replicates were performed, and similar results were obtained.

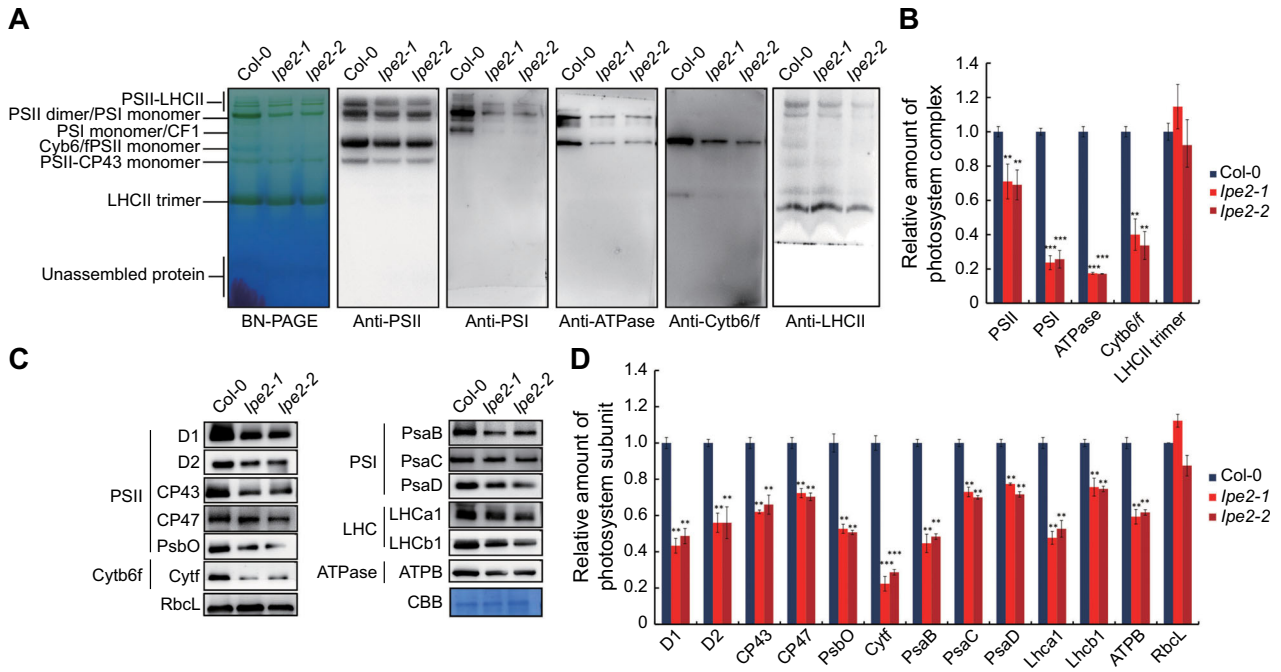

Figure 3. Analysis of photosystem complexes and subunits from the wild-type (WT) and *LOW PHOTOSYNTHETIC EFFICIENCY2 (lpe2)* mutant plants

(**A**) Blue native-polyacrylamide gel electrophoresis (BN-PAGE) and immunoblot analysis of chlorophyll-protein complexes. Equal thylakoid membranes (10 μg of chlorophyll) from the leaves of the wild type and *lpe2* mutants were solubilized by treatment with 2% (w/v) dodecyl b-D-maltoside and separated by BN-PAGE. The assignments of the macromolecular protein complexes of thylakoid membranes indicated at left were identified according to Jin et al. (2014). then BN-PAGE (3 μg of chlorophyll) for immunoblot analysis, Anti-D1 antiserum used to probe the PSII complex, anti-PsaA antiserum used to probe the PSI complex, anti-cytochrome f antiserum used to probe the cytochrome b6/f (Cytb6/f) complex, anti-ATPB antiserum used to probe the ATP synthase (ATPase) complex. anti-Lhca1 antiserum used to probe the light harvesting complex II (LHCII) trimer complex. Three independent biological replicates for all experiments were performed, and a representative one is shown. The LHCII trimmer is used as a control. (**B**) Proteins immunodetected from (**A**) were analyzed with Phoretix 1D Software (Phoretix International). Values (means ± *SE*; $n = 3$ independent biological replicates) are given as ratios to protein amounts of the wild type (Col-0) and *lpe2* mutants. **, $P < 0.01$;***, $P < 0.001$, by Student's *t*-test. (**C**) Thylakoid membrane proteins from the wild type (Col-0) and *lpe2* mutants were separated by 12% SDS-urea-PAGE, transferred onto polyvinylidene difluoride membranes, and probed with antibody against known thylakoid membrane proteins obtained from Agrisera. Samples were loaded on an equal chlorophyll basis. Cytf, Cytochrome b6/f complex; LHC, light-harvesting complex; ATPase, ATP synthase complex. CBB, Coomassie brilliant blue. Rubisco large subunit (RbcL) is used as a control. (**D**) Proteins immunodetected from (**C**) were analyzed with Phoretix 1D Software (Phoretix International). Values (means ± *SE*; $n = 3$ independent biological replicates) are given as ratios to protein amounts of the wild type (Col-0) and *lpe2* mutants. **, $P < 0.01$;***, $P < 0.001$, by Student's *t*-test. All experiments were repeated three times with similar results.

of gene expression in the *lpe2* mutant, transcripts of plastid-encoded genes involved in PSII (*psbA*, *psbB*, *psbC*, and *psbD*), PSI (*psaA*, *psaB*, and *psaC*), ATPase (*atpA*, *atpB*, *atpE*, and *atpF*), and Cytb6/f (*petA*, *petB*, *petD*, and *petG*) were tested by quantitative real-time PCR (qRT-PCR) (Figure S1). No dramatic differences in gene expression were observed between the *lpe2* mutants and WT plants. Thus, the *lpe2* mutation did not affect photosynthesis-related genes at the transcriptional level, suggesting that the mutation affected these genes at the post-transcriptional level.

Absence of LPE2 alters the expression of nuclear genes

To determine whether defects of protein synthesis caused by LPE2 deficiency alter expression of nuclear genes, the transcriptome of *lpe2* mutant and WT

plants were determined using RNA-Seq. A volcano plot showed hierarchical clustering of DEGs in *lpe2* and Col-0 plants in two biological replicates (Figure 4A). A total of 562 differentially expressed genes (DEGs) were detected from the comparison between WT and *lpe2* mutant plants (Figure 4A; Table S2). Of these, 142 DEGs were upregulated and 420 were downregulated. In both biological replicates, the majority of the DEGs exhibited similar expression patterns, thus showing consistent upregulation or downregulation (Figure 4A).

To functionally annotate the DEGs, we aligned all DEGs against the Kyoto Encyclopedia of Genes and Genomes (KEGG) and Gene Ontology (GO) databases. GO analysis classified the DEGs into three major GO categories: cell component, molecular function, and biological process. The most abundant category is biological process, followed by molecular function, and cell component (Figures 4B, S2). Results of KEGG analysis indicated that DEGs were involved in 72 pathways, of which the top 30 pathways are presented in Figure 4B, including sugar (C) metabolism and signaling, nitrogen (N) metabolism and signaling, redox regulation, hormone synthesis, root development, ion transport, response to mechanical stimulus, pigment metabolism, etc.

Loss of LPE2 alters C and N response

Among the nuclear-encoded DEGs described above, we focused on C and N response-related genes. According to the results of GO analysis, 13 pathways were involved in C metabolism and signaling, and three pathways were involved in N metabolism and signaling (Figure 5A–E). Notably, genes involved in C metabolism (*SWEET14*, *TGG5*, and *BGLU22*) and N metabolism (*NPF2.4*, *NPF2.5*, and *NPF1.2*) were downregulated in the *lpe2* mutant compared with the WT (Figure 5B, E). These results imply a potential role of LPE2 in the response to C/N balance. Furthermore, qRT-PCR analysis of these genes using gene-specific primers verified the RNA-Seq data; compared with the WT, all six genes were downregulated in *lpe2* mutant plants (Figure 5C, F).

Response to C/N balance is suppressed in *lpe2* mutants

Previously, studies reported crosstalk between N-responsive and C-responsive pathways (Coruzzi and Bush 2001; Coruzzi and Zhou 2001), and C/N balance has been shown to regulate the expression of carbohydrate and N related genes (Lejay et al. 1999; Oliveira and Coruzzi 1999; Zhuo et al. 1999; Zheng 2009). The loss of LPE2 confers C and N response, which suggests

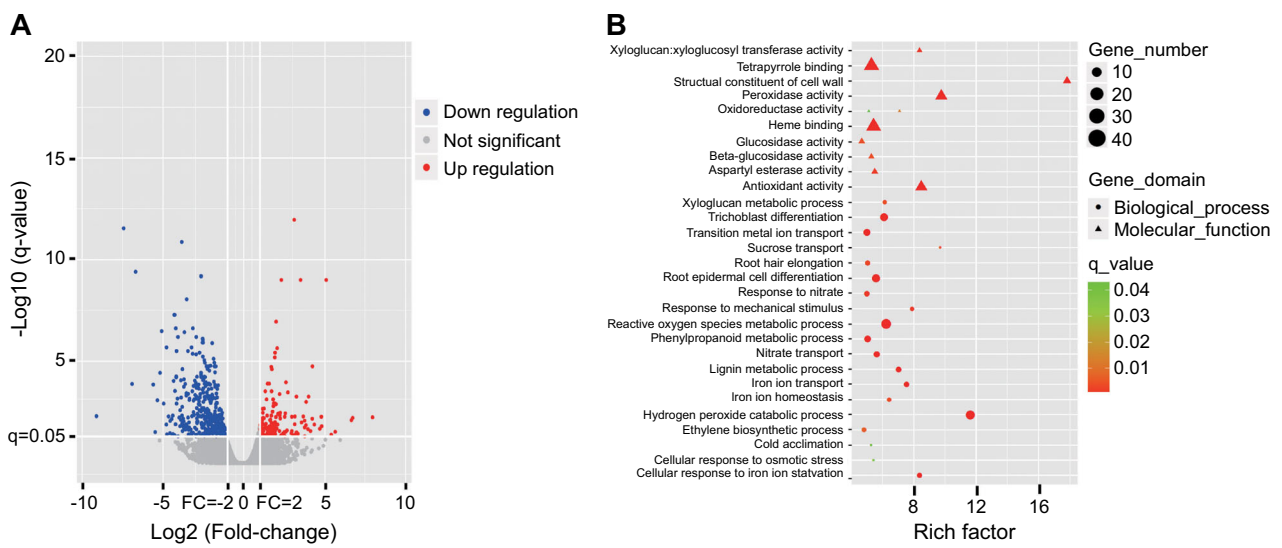

Figure 4. Transcriptome analysis of wild-type (WT) and *LOW PHOTOSYNTHETIC EFFICIENCY2 (lpe2)* mutant plants
(**A**) Volcano plot showing difference of gene expression in *lpe2-2* mutant plants plotted against −log10 (q-value) highlighting wild type plants (dark grey, q-value < 0.05, $n = 3$, ANOVA). Blue plots indicate down regulation; red plots indicate up regulation; gray plots indicate not significant. (**B**) Analysis of differentially expressed genes (DEGs). The enriched molecular function terms of DEGs among wild type and *lpe2-2* mutant plants. Two additional independent biological replicates were performed, and similar results were obtained.

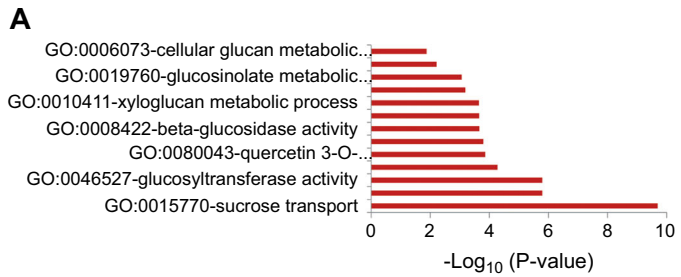

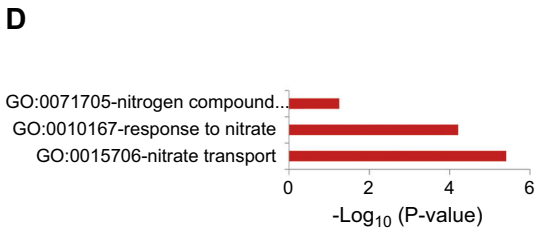

B

Gene ID	Gene name	Log2FC	P value	Q value	Up/Down
AT4G25010	SWEET14	-3.23795	0.000664862	0.033707	Down
AT1G51470	TGG5	-3.5359	0.00075372	0.00065535	Down
AT1G66280	BGLU22	-1.75964	0.00000375	0.000655	Down

E

Gene ID	Gene name	Log2FC	P value	Q value	Up/Down
AT3G45700	NPF2.4	-2.56658	0.000191	0.013682	Down
AT3G45710	NPF2.5	-1.58721	0.000344	0.020761	Down
AT1G52190	NPF1.2	-1.41594	1.92E-05	0.002472	Down

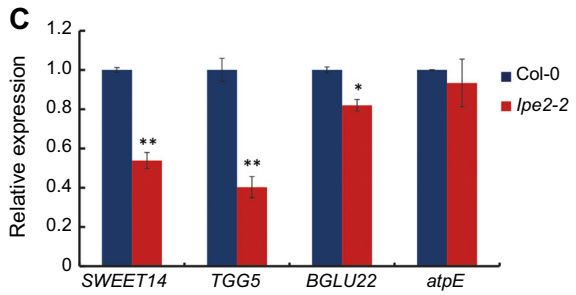

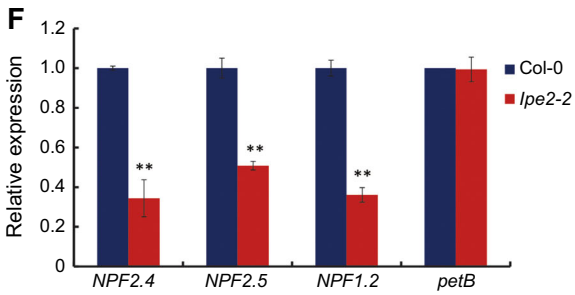

Figure 5. Loss of LOW PHOTOSYNTHETIC EFFICIENCY2 (LPE2) confers carbon-response and nitrogen-response
(**A**) Gene Ontology (GO) analysis of genes relative to carbon metabolism and signal in the transcriptome data. (**B**) Downregulated genes relative to carbon metabolism and signal. (**C**) Relative levels of expression of genes associated with carbon metabolism and signal in Col-0 and *lpe2-2*. Values are means ± *SD* from three biological replicates. The *atpE* gene is used as a control. (**D**) GO analysis of genes relative to nitrogen metabolism and signal. (**E**) Downregulated genes relative to nitrogen metabolism and signal in the transcriptome data. (**F**) Relative levels of expression of genes associated with nitrogen metabolism and signal in Col-0 and *lpe2-2*. Values are means ± *SD* from three biological replicates. The *petB* gene is used as a control.

a potential role of LPE2 in C/N stress responses. To verify this assumption, we compared the phenotype of WT and *lpe2* mutant plants grown on modified Murashige and Skoog (MS) medium containing different concentrations of sucrose and nitrogen (Figures 6A, S3). In the presence of normal medium (29.2S/60N), WT seedlings exhibited normal green cotyledons. No significant change was observed in the phenotypes of mutant vs. WT plants when we reduced the concentration of sucrose and nitrogen (0S/0.1N). By contrast, at high N concentration (0S/60N), WT plants were much bigger than *lpe2* mutant and produced primary leaves. Under normal growth conditions, increasing the Suc concentration to 100 mM (100S/60N) resulted in a slightly larger plant size and the production of primary leaves. When the N concentration was decreased to 0.1 mM (100S/0.1N), WT plants showed strong post-germination growth arrest and purple pigmentation. The response of *lpe2* seedlings post-germination to changes in C/N balance was much more subtle than that of WT seedlings. When grown in the normal medium (29.2S/60N), *lpe2* seedlings were smaller than WT seedlings; however, the size of *lpe2* and WT seedlings showed no obvious difference. when the sucrose concentration was reduced to zero (0S/60N), *lpe2* seedlings were slightly smaller in size than WT seedlings. Additionally, the effect of high C and low N on plant growth was much less severe in the *lpe2* mutant than in the WT; *lpe2* plants showed post-germination and cotyledon expansion growth under these conditions. These results indicate that *lpe2* plants has reduced sensitivity to changes in C/N balance during post-germinative growth (Figures 6A, S3).

To further assess the response of *lpe2* mutants to C/N balance, we examined transcript levels of three marker

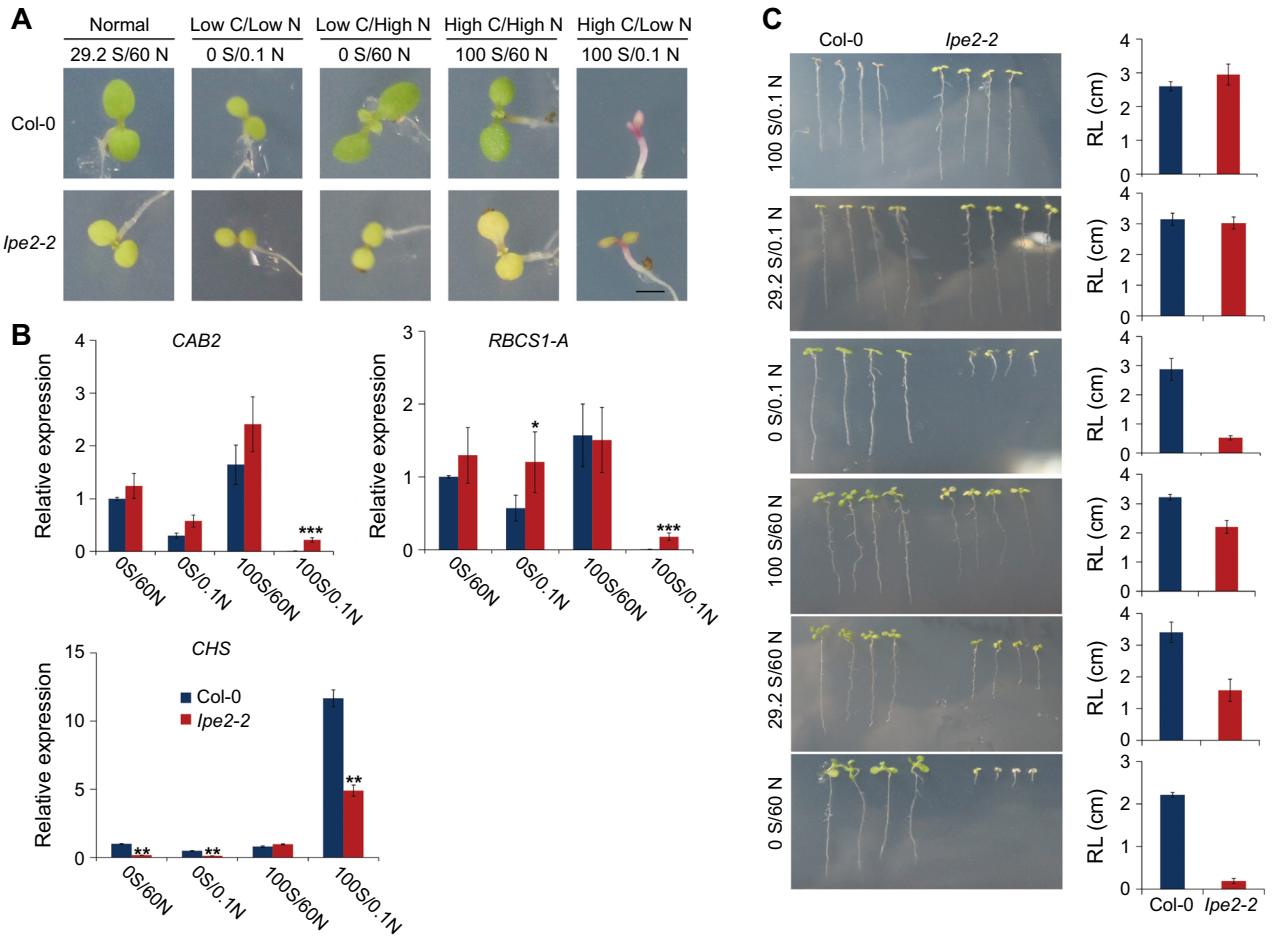

Figure 6. ***LOW PHOTOSYNTHETIC EFFICIENCY2 (LPE2) deficiency*** **suppressed carbon/nitrogen (C/N) response**
(**A**) Phenotypes of *Arabidopsis* seedlings germinated and grown for 7 d on media containing different concentrations of Suc and nitrogen.100 Suc/0.1 N, 100 mM Sucrose and 0.1 mM nitrogen; 100 Suc/60 N, 100 mM Sucrose and 60 mM nitrogen; 29.2 Suc/60 N, 29.2 mM Sucrose and 60 mM nitrogen;0 Suc/0.1 N, 0 mM Sucrose and 0.1 mM nitrogen; 0 Suc/60 N, 0 mM Sucrose and 60 mM nitrogen. Scale bar = 0.1 cm. 29.2 Suc/60 N medium indicate the normal concentration of C and N in 1/2 MS. Bar = 0.3 cm. (**B**) Quantitative real-time polymerase chain reaction (qRT-PCR) analysis of *CAB2*, *RBCS1-A* and *CHS* mRNA transcript levels in wild-type (WT) and *lpe2* seedlings. Each line was germinated on the same media variations as described in (**A**), and then analyzed 7 d after germination. Significant differences were identified at 5% (*) and 1% (**) probability levels by using Student's *t*-test. (**C**) Root length of *Arabidopsis* seedlings germinated and grown for 10 d on media containing different concentrations of Suc and nitrogen. 100 Suc/0.1 N, 100 mM Sucrose and 0.1 mM nitrogen; 100 Suc/60 N, 100 mM Sucrose and 60 mM nitrogen; 29.2 Suc/0.1 N, 29.2 mM Sucrose and 0.1 mM nitrogen; 29.2 Suc/60 N, 29.2 mM Sucrose and 60 mM nitrogen;0 Suc/0.1 N, 0 mM Sucrose and 0.1 mM nitrogen; 0 Suc/60 N, 0 mM Sucrose and 60 mM nitrogen. Scale bar = 0.1 cm. 29.2 Suc/60 N medium indicate the normal concentration of C and N in 1/2 MS. Three additional independent biological replicates were performed, and similar results were obtained.

genes affected by availability of C/N (Figure 6B). The genes encoding small subunit of Rubisco (RBCS1-A) and chlorophyll a/b-binding protein (CAB2) are downregulated by a high C:N ratio (Martin et al. 2002). The anthocyanin biosynthesis related gene chalcone synthase (*CHS*) is up-regulated by a high C:N ratio (Martin et al. 2002). As expected, the transcripts of *RBCS1-A* and *CAB2* genes accumulated in WT seedlings on both medium combinations lacking sucrose. Transcripts of *RBCS1-A* and *CAB2* also obviously accumulated in WT seedlings grown in the presence of 100 mM C and 60 mM N but not in WT seedlings grown under high C/N conditions (100S/0.1N). In *lpe2* seedlings, *RBCS1-A* and *CAB2* transcripts were detected in response to all combinations of C and N

concentrations. After high C/N (100S/0.1N) treatment, *CHS* transcripts accumulated to high levels in WT seedlings significantly but not in *lpe2* seedlings (Figure 6B). These results suggest that *lpe2* is less sensitive to C/N conditions, and the regulation of the response of *lpe2* mutants to C/N balance for post-germination growth arrest is disrupted.

We further observed the response of *lpe2* to C/N growth conditions in the root growth assay (Figure 6C). When grown in medium containing 29.2 mM sucrose and 60 mM N (29.2S/60N), *lpe2* seedlings displayed shorter roots than WT seedlings. When we increased the sucrose concentration or decreased the N concentration, the difference between the root length of *lpe2* and Col-0 plants declined. Additionally, when C and N concentrations were simultaneously increased and reduced, respectively, *lpe2* roots were longer than Col-0 roots. However, when the concentration of sucrose or N was reduced, the root length of *lpe2* was much shorter than that of WT. These results further support that LPE2 deficiency suppresses the response to C/N balance. More interestingly, we found that levels of *LPE2* expression in the conditions of 100C/1N, 0S/60N, 0S/0.1N, were 95%, 91%, 68% lower than that in the normal conditions (29.2S/60N). However, levels of *LPE2* expression in the conditions of 100S/60N is comparable to that in the normal conditions (29.2S/60N) (Figure S4). These results suggest that both C and N deficiency can depress the expression of *LPE2* genes, which can be aggravated by higher C/N ratio. More interestingly, the expression pattern of *LPE2* gene and is similar to that of *CAB2* and *RBCS1-A* in the different C/N conditions (Figure S4).

DISCUSSION

Plastid RPs are key constituents of the translation machine of plastids, and is required for normal plant growth and development. Despite the increasing number of studies conducted on plastid RPs (Pesaresi et al. 2001; Romani et al. 2012; Gong et al. 2013; Ma et al. 2015; Tadini et al. 2016; Zhang et al. 2016), the effect of plastid RPs on plant growth and development is not well understood, and the roles of some RPs remain largely unknown. This study identified two loss-of-function mutant alleles of *LPE2*, which is predicted to encode a plastid RP, namely, S21 (Figure 1). It was suggested that LPE2 is involved in glucose response during seed germination in *Arabidopsis* (Morita-Yamamuro et al. 2004). In this study, we confirmed that LPE2 plays an important role in plastid ribosome function, and is required for photosynthesis and response to C/N balance in *Arabidopsis.*

RPs are critical for protein translation in plastids, and the absence of RPs affects plant development. Both *lpe2-1 and lpe2-2* mutants showed similar phenotypes, including pale green cotyledons, small plant size, and low photosynthetic activity, confirming that these phenotypes are resulted from the LPE2 deficiency (Figure 1). Furthermore, our results revealed that the *lpe2* mutation perturbed thylakoid composition and plastid protein accumulation but not transcription of plastid gene, which suggests that LPE2 is involved in photosynthesis and support the functions as a plastid RP (Figures 3, S1). Similar to cytoplasmic RPs, the absence of a single plastid RP causes defects in specific stages of plant development (Zsogon et al. 2014). For example, the lack of PRPS5, PRPS13, PRPS20, PRPL1, PRPL4, PRPL6, PRPL21, PRPL27, and PRPL35 disturb the transition of embryo from the globular to the heart stage (Bryant et al. 2011; Lloyd and Meinke 2012; Zhang et al. 2016). PRPL28 is required for the transition from the embryos to greening of seedlings, whereas PRPS1, -L24, -L11, -S21, and -S17 are crucial for maintaining the activity and function of ribosomes in adult plants (Pesaresi et al. 2001; Morita-Yamamuro et al. 2004; Romani et al. 2012; Tiller et al. 2012). The *LPE2* gene is expressed at all stages of plant growth, and shows high expression in rosette leaves (Morita-Yamamuro et al. 2004). The results in this study verified that LPE2 have a vital role in adult plants although the lack of LPE2 can finish the whole plant life cycle.

Several studies suggest that the deficiency of RPs induces stress response via retrograde signaling from plastids to nucleus. For example, *Arabidopsis* knockdown mutant *rps1* inhibits heat stress response by regulating heat-responsive transcriptional activation of *HsfA2* (*HEAT SHOCK TRANSCRIPTION FACTOR A2*) (Yu et al. 2012). It is reported that the *rps5* mutation suppresses the expression of genes encoding a large number of PSI and PSII core components as well as many plastid RPs. Many cold stress response proteins are decreased in *rps5* mutant greatly, and the overexpression of plastid *RPS5* improves cold stress tolerance of plants (Zhang et al. 2016). In this study, gene

expression analysis showed that the *lpe2* mutation generated a retrograde signal, thus altering the expression of several different kinds of genes (Figure 4), including those involved in C and N response (Figure 5). Since the expression of C and N response genes is regulated by C/N balance (Oliveira and Coruzzi 1999; Martin et al. 2002; Maruta et al. 2015), our data suggest that LPE2 is also involved in C/N balance. This was supported by the C/N stress test, in which the loss of LPE2 suppressed C/N response (Figure 6).

Plants are often grown in nutrient-deficient soil. To adapt to nutrient-deficient conditions, plants have developed strategies that adjust gene expression in nucleus to response it. The C and N are important nutrients required for plant growth, and their levels must be regulated tightly to optimize plant growth and development. Therefore, C/N balance is essential for regulating the expression of C and N related genes (Lejay et al. 1999; Oliveira and Coruzzi 1999; Zhuo et al. 1999). A few proteins have been reported to play vital roles in C/N balance: NRT2.1 (NITRATE TRANSPORTER 2.1) plays a role in the initiation of lateral roots in response to C/N balance (Little et al. 2005; Remans et al. 2006); putative glutamate receptor GLR1.1 shows sensitivity to abscisic acid (ABA) under high sucrose/low nitrate conditions (Kang and Turano 2003); OSU1/QUA2/TSD2 (QUASIMODO2) is involved in pectin biosynthesis and response to C/N balance (Gao et al. 2008); and ATL31 (ARABIDOPSIS TOXICOS EN LEVADURA 31), which is a ubiquitin ligase, regulates C/N balance (Sato et al. 2009). Thus, C/N response is triggered by different biological factors such as developmental, environmental conditions cell type, and/or metabolic (Coruzzi and Zhou 2001). Here, we identified LPE2 as a novel factor influencing the C/N balance. The expression pattern of *LPE2* gene is similar to that of *CAB2* and *RBCS1-A* in the different C/N conditions (Figure S4). The loss of LPE2 suppressed the response to C/N balance, as shown by a wide range of phenotypic and molecular data under high C/low N conditions (Figure 6). Our findings indicate LPE2 may functions as a key genetic connection between the translation capacity of chloroplasts and transcriptional regulation of C/N-responsive genes. However, we did not completely rule out the indirect effect of chloroplast dysfunction of *lpe2* mutants on the response to C/N balance, such as light reaction, dark reaction or other metabolisms in chloroplasts. Previous study reported that pHXK which is a plastid hexokinase functions as the junction for sugar and plastid signals in *Arabidopsis* (Zhang et al. 2010). However, the nitrogen response and C/N balance regulated by chloroplast have not been reported. This study suggest that LPE2 probably mediates a retrograde signaling from plastid to nucleus to regulate the C/N balance, although the mechanism of regulation need to be further clarified.

MATERIALS AND METHODS

Plant materials and growth conditions

Arabidopsis T-DNA insertion mutant lines in Col-0 background were used in this study. The *lpe2-1* (SALK_077692) and *lpe2-2* (CS843433) mutants were obtained from the *Arabidopsis* Biological Resource Center (ABRC), The Ohio State University, OH, USA. Plants were grown in soil in a growth chamber under controlled conditions (21°C temperature, 60% relative humidity, 12 h light/12 h dark photoperiod, and 100 μmol photons m^2/s light intensity). Three- and four-week-old plants were used for chlorophyll fluorescence assays and protein analysis, respectively. For plants grown on agar plates, we use 75% ethanol (1 min) and 20% blench (15 min) to sterilize and sown on 1/2 MS medium (Phyto Technology Laboratories), which is added with 1% (w/v) sucrose and 1% (w/v) agar. Subsequently, we put the plates at 4°C (darkness) for 3 d to vernalize the seeds and transferred it to a growth chamber.

Assay for determining the response to C/N balance

Surface-sterilized seeds of *Arabidopsis lpe2* mutants and Col-0 were sown on 1/2MS medium (Murashige and Skoog 1962) containing different proportions of sugar and N. The ratio of potassium nitrate (KNO_3) to ammonium nitrate (NH_4NO_3) in each experiment was maintained (Murashige and Skoog 1962). Potassium chloride (KCl) was added to the medium to compensate for the lower K^+concentration in reduced KNO_3-containing media, as reported (Sato et al. 2009).

Generation of anti-LPE2 polyclonal antibodies

Affinity-purified anti-LPE2 polyclonal antibodies were prepared by GenScript. A 15-amino-acid peptide (corresponding to amino acids 137–151 of LPE2) with an

additional N-terminal Cys residue, CAAKRNKKRRP-QARF, was synthesized, conjugated with keyhole limpet hemocyanin, and used to induce antibodies against LPE2 in rabbits.

Measurement of chlorophyll fluorescence

Chlorophyll fluorescence parameters were measured using the MAXI version of the IMAGING-PAM M-Series chlorophyll fluorescence system (Heinz-Walz Instruments). Three-week-old plants were used for chlorophyll fluorescence assays. Plants were dark adapted for 30 min prior to measurements, and the maximum fluorescence yield was determined by applying a saturating light pulse (3×10^3 µmol photons m^2/s). Thereafter, the maximal fluorescence of light adapted leaves was measured after applying a second saturating pulse. The light response curves were determined as described previously (Jin et al. 2018). Light-response curves of PSII quantum yield (ΦPSII), non-photochemical quenching (qN), and electron transport rate (ETR) were measured every 3 min at the following light intensities: 0, 81,145, 186, 281, 335, 461, 701, and 926 µmol photons m^2/s. Each data point represents at least 20 independent plants.

Isolation of thylakoid membranes

Thylakoid membranes were isolated as described by Suorsa et al. (2006) with minor modifications. Buffer was prepared before the experiment, which containing 20 mM Tricine-KOH (pH 8.0), containing 2 mM $MgCl_2$, 1 mM $NaVO_3$, 0.4 M NaCl,10 mM NaF and 0.2% bovine serum albumin and put it in ice. Mature leaves (4 weeks old) were excised and grounded in this buffer, then blended quickly. Next, filtered the resulting lysate through four layers of cheesecloth into 50 mL centrifuge tubes and centrifuged these tubes for 10 s at 800 g at 4°C. The suspension was transferred to another centrifuge tube and centrifuged for 10 min at 4000 g at 4°C. The pellet was resuspended and centrifuged in buffer containing 20 mM Tricine-KOH(pH8.0), 0.15 M NaCl, 5 mM $MgCl_2$, 0.2% bovine serum albumin, 1 mM $NaVO_3$, and 10 mM NaF. The thylakoid pellet was resuspended and centrifuged twice as above. The final pellet was resuspended in buffer containing 20 mM Tricine-KOH (pH8.0),15 mM NaCl, 0.4 mM sucrose, 0.2% bovine serum albumin, 10 mM NaF, and 10 mM NaF 1 mM $NaVO_3$ in a small volume.

Quantitative real-time polymerase chain reaction analysis

Total RNA was extracted from fifth to seventh rosette leaves of 4-week-old plants *lpe2* mutant and WT plants (0.5 g leaves for each experiment) using RNeasy Plant Mini Kit (Qiagen), and reverse transcribed for the synthesis of first strand complementary DNA (cDNA) using PrimeScript RT reagent kit (Takara). The cDNA was amplified by qRT-PCR using gene-specific primers (Table S1) and SYBR Premix Ex*Taq* reagent (Takara) with a real-time RT-PCR system (RoChe-LC480), according to the manufacturer's instructions. Three-time repetition was performed and normalized relative to the *ACTIN* gene for each example.

Blue native-polyacrylamide gel electrophoresis and immunoblot analyses

The fifth to eighth leaves of 4 weeks old plants (1 g leaves for each experiment) were used for protein analysis. Blue native-polyacrylamide gel electrophoresis was performed as described previously (Schagger et al. 1994), on the basis of it, did some modifications (Peng et al. 2006). To quantify thylakoid proteins, samples containing equal amounts of chlorophyll were loaded on a gel, while ensuring a linear range for immune detection. Thylakoid preparations made as the above description were solubilized with 2% (w/v) dodecyl b-D-maltoside (Sigma) for 20 min (on ice). Electrophoresis was performed using Native PAGE 5–12% Bis-Tris gel at 4°C. For immunoblot analysis, add the protein extract buffer in leaves or thylakoid membrane preparations, grinded the leaves and centrifuged, then separated on 12% SDS-PAGE gels with 6 M urea. After electrophoresis, total or thylakoid proteins were transferred to polyvinylidene difluoride membranes (Millipore) and probed using antibodies. Antibody against photosynthetic proteins were purchased from Agrisera. All primary antibodies and antisera used in this study were produced in rabbits. Signals were detected with the SuperSignal West Pico Chemiluminescent Substrate (Thermo Scientific).

Subcellular localization of GFP fusion proteins

Subcellular localization of GFP fusion proteins contains two steps, *Arabidopsis* protoplast preparation and transfer plasmid into proplast. The preparatory work of protoplast was done as previously described (Zhai et al. 2009). Fourteen days old *Arabidopsis*

leaves were cut into small pieces in TVL solution (50 mM $CaCl_2$ and 0.3 M sorbitol) and used enzyme solution (0.5 M sucrose,1% Macerozyme R-10,20 mM $CaCl_2$, 1% Cellulase R-10, 40 mM KCl, and 10 mM MES-KOH (pH5.7)) to incubate with gentle shaking for 6 h (dark). Then centrifuged to collect the protoplasts (100 g for 7 min) and used W5 solution (1.84% $CaCl_2$, 0.1% glucose, 2 mM MES (pH 5.7), 0.9% NaCl, and 0.08% KCl) to wash twice. For GFP analyses, 10 μg LPE2-GFP plasmid DNA add to 100 μL (~10^4 cells) *Arabidopsis* protoplasts to transfection. As a positive control, HHL1-GFP (HYPERSENSITIVE TO HIGH LIGHT 1) was transfected into protoplasts (Jin et al. 2014). Then incubation for 12 h, the GFP fluorescence was captured by confocal microscope (TCS-SP5; Leica) as previously described (Yuan et al. 2008).

Chloroplast isolation and fractionation

Thylakoid and stroma phases were separated as described (Armbruster et al. 2010). Three weeks old leaves were ground in 330 mM sorbitol, 10 mM Na_2CO_3, 20 mM Tricin-NaOH(pH 7.6), 0.1% (w/v) bovine serum albumin (BSA), 5 mM EGTA and 330 mg/L ascorbate, then filtered and centrifuged for 5 min (2,000 g). Then used the buffer with 330 mM sorbitol, 0.1% (w/v) BSA,10 mM Na_2CO_3, 20 mM HEPES-KOH (pH 7.6), 2.5 mM EDTA, 10 mM Na_2CO_3 and 5 mM $MgCl_2$ to resuspended the pellet, and isolated the intact chloroplasts though a 40/70% step Percoll gradient. then used the buffer with 0.3 M sorbitol, 20 mM Hepes-KOH(pH 8), 5 mM $MgCl_2$, 5 mM EGTA, 5 mM Na_2EDTA, 20 mM Hepes-KOH(pH 8) and 10 mM $NaHCO_3$ to wash twice and used the breaking buffer (10 mM $MgCl_2$, and 50 mM Hepes-KOH(pH 8)) to disrupt. The stromal and membrane fractions were separated by centrifugation 20,000 *g* for 20 min can make the stromal and membrane fraction separate.

RNA-sequencing and data analysis

Seedlings grown in 1/2MS for two weeks were collected for RNA-sequencing analysis, each sample containing two biological replicates. RNAiso Plus (TaKaRa Code:D9108A) was used to extract total RNAs, part of the RNA was used to transcription expression analysis by Shanghai Biotechnology Corporation, and the other part of it was used to qRT-PCR to verify the results. mRNA-Seq Sample Preparation Kit (Illumina) was used for library construction and there was about 45 bp inserted into the library. Every transcript's FPKM value was calculated by Cufflinks (version: 2.0.23). The Fisher's exact test was used to calculate the *P*-value. the significant difference threshold was $P < 0.05$ and the absolute value of $\log2FC \geq 0.585$ (Trapnell et al. 2010). For pathway analysis, MapMan package was used to map all different expression genes with the ensemble mapping file (Thimm et al. 2004). Volcano plots Ggrepel packages was used to make volcano plot.

ACKNOWLEDGEMENTS

We thank ABRC for providing plant materials. This research was supported by grants from the National Natural Science Foundation of China (31770260 and 31970261), and National Science Fund for Distinguished Young Scholars of China (31425003).

AUTHOR CONTRIBUTIONS

H.L.J. and X.D. designed and conducted the research. H.J. and X.D. performed research. H.L.J. and X.D. wrote the manuscript. H.B.W. and S.D. revised the manuscript. All authors read and approved the manuscript.

REFERENCES

Albrecht V, Ingenfeld A, Apel K (2006) Characterization of the snowy cotyledon 1 mutant of *Arabidopsis thaliana*: The impact of chloroplast elongation factor G on chloroplast development and plant vitality. **Plant Mol Biol** 60: 507–518

Andriankaja M, Dhondt S, De Bodt S, Vanhaeren H, Coppens F, De Milde L, Muhlenbock P, Skirycz A, Gonzalez N, Beemster GT, Inze D (2012) Exit from proliferation during leaf development in *Arabidopsis thaliana*: A not-so-gradual process. **Dev Cell** 22: 64–78

Armbruster U, Zuhlke J, Rengstl B, Kreller R, Makarenko E, Ruhle T, Schunemann D, Jahns P, Weisshaar B, Nickelsen J, Leister D (2010) The *Arabidopsis* thylakoid protein PAM68 is required for efficient D1 biogenesis and photosystem II assembly. **Plant cell** 22: 3439–3460

Baba K, Schmidt J, Espinosa-Ruiz A, Villarejo A, Shiina T, Gardestrom P, Sane AP, Bhalerao RP (2004) Organellar gene transcription and early seedling development are

affected in the rpoT;2 mutant of *Arabidopsis*. **Plant J** 38: 38–48

Babiychuk E, Vandepoele K, Wissing J, Garcia-Diaz M, De Rycke R, Akbari H, Joubes J, Beeckman T, Jansch L, Frentzen M, Van Montagu MC, Kushnir S (2011) Plastid gene expression and plant development require a plastidic protein of the mitochondrial transcription termination factor family. **Proc Natl Acad Sci USA** 108: 6674–6679

Bryant N, Lloyd J, Sweeney C, Myouga F, Meinke D (2011) Identification of nuclear genes encoding chloroplast-localized proteins required for embryo development in *Arabidopsis*. **Plant Physiol** 155: 1678–1689

Chan KX, Phua SY, Crisp P, McQuinn R, Pogson BJ (2016) Learning the languages of the chloroplast: Retrograde signaling and beyond. **Annu Rev Plant Biol** 67: 25–53

Coruzzi G, Bush DR (2001) Nitrogen and carbon nutrient and metabolite signaling in plants. **Plant Physiol** 125: 61–64

Coruzzi GM, Zhou L (2001) Carbon and nitrogen sensing and signaling in plants: Emerging 'matrix effects'. **Curr Opin Plant Biol** 4: 247–253

Emanuelsson O, Nielsen H, Brunak S, von Heijne G (2000) Predicting subcellular localization of proteins based on their N-terminal amino acid sequence. **J Mol Biol** 300: 1005–1016

Estavillo GM, Crisp PA, Pornsiriwong W, Wirtz M, Collinge D, Carrie C, Giraud E, Whelan J, David P, Javot H, Brearley C, Hell R, Marin E, Pogson BJ (2011) Evidence for a SAL1-PAP chloroplast retrograde pathway that functions in drought and high light signaling in *Arabidopsis*. **Plant Cell** 23: 3992–4012

Feng P, Guo H, Chi W, Chai X, Sun X, Xu X, Ma J, Rochaix JD, Leister D, Wang H, Lu C, Zhang L (2016) Chloroplast retrograde signal regulates flowering. **Proc Natl Acad Sci USA** 113: 10708–10713

Gao P, Xin Z, Zheng ZL (2008) The OSU1/QUA2/TSD2-encoded putative methyltransferase is a critical modulator of carbon and nitrogen nutrient balance response in *Arabidopsis*. **PLoS ONE** 3: e1387

Garcia M, Myouga F, Takechi K, Sato H, Nabeshima K, Nagata N, Takio S, Shinozaki K, Takano H (2008) An *Arabidopsis* homolog of the bacterial peptidoglycan synthesis enzyme MurE has an essential role in chloroplast development. **Plant J** 53: 924–934

Gong X, Jiang Q, Xu J, Zhang J, Teng S, Lin D, Dong Y (2013) Disruption of the rice plastid ribosomal protein s20 leads to chloroplast developmental defects and seedling lethality. **G3** 3: 1769–1777

Hernandez-Verdeja T, Strand A (2018) Retrograde signals navigate the path to chloroplast development. **Plant Physiol** 176: 967–976

Hsu SC, Belmonte MF, Harada JJ, Inoue K (2010) Indispensable Roles of Plastids in *Arabidopsis thaliana* Embryogenesis. **Curr Genomics** 11: 338–349

Jin H, Fu M, Duan Z, Duan S, Li M, Dong X, Liu B, Feng D, Wang J, Peng L, Wang H-B (2018) LOW PHOTOSYNTHETIC EFFICIENCY 1 is required for light-regulated photosystem II biogenesis in *Arabidopsis*. **Proc Natl. Acad Sci** 115: E6075–E6084

Jin H, Liu B, Luo L, Feng D, Wang P, Liu J, Da Q, He Y, Qi K, Wang J, Wang HB (2014) HYPERSENSITIVE TO HIGH LIGHT1 interacts with LOW QUANTUM YIELD OF PHOTOSYSTEM II1 and functions in protection of photosystem II from photodamage in Arabidopsis. **Plant cell** 26: 1213–1229

Kang J, Turano FJ (2003) The putative glutamate receptor 1.1 (AtGLR1.1) functions as a regulator of carbon and nitrogen metabolism in *Arabidopsis thaliana*. **Proc Natl Acad Sci USA** 100: 6872–6877

Kleine T, Voigt C, Leister D (2009) Plastid signalling to the nucleus: Messengers still lost in the mists? **Trends Genet** 25: 185–192

Lejay L, Tillard P, Lepetit M, Olive F, Filleur S, Daniel-Vedele F, Gojon A (1999) Molecular and functional regulation of two NO^{3-} uptake systems by N- and C-status of *Arabidopsis* plants. **Plant J** 18: 509–519

Leon P, Arroyo A, Mackenzie S (1998) Nuclear control of plastid and mitochondrial development in higher plants. **Annu Rev Plant Physiol Plant Mol Biol** 49: 453–480

Lin D, Jiang Q, Zheng K, Chen S, Zhou H, Gong X, Xu J, Teng S, Dong Y (2015) Mutation of the rice *ASL2* gene encoding plastid ribosomal protein L21 causes chloroplast developmental defects and seedling death. **Plant Biol** 17: 599–607

Little DY, Rao H, Oliva S, Daniel-Vedele F, Krapp A, Malamy JE (2005) The putative high-affinity nitrate transporter NRT2.1 represses lateral root initiation in response to nutritional cues. **Proc Natl Acad Sci USA** 102: 13693–13698

Lloyd J, Meinke D (2012) A comprehensive dataset of genes with a loss-of-function mutant phenotype in *Arabidopsis*. **Plant Physiol** 158: 1115–1129

Ma Z, Wu W, Huang W, Huang J (2015) Down-regulation of specific plastid ribosomal proteins suppresses thf1 leaf variegation, implying a role of THF1 in plastid gene expression. **Photosynth Res** 126: 301–310

Martin T, Oswald O, Graham IA (2002) *Arabidopsis* seedling growth, storage lipid mobilization, and photosynthetic gene expression are regulated by carbon: Nitrogen availability. **Plant Physiol** 128: 472–481

Maruta T, Miyazaki N, Nosaka R, Tanaka H, Padilla-Chacon D, Otori K, Kimura A, Tanabe N, Yoshimura K, Tamoi M, Shigeoka S (2015) A gain-of-function mutation of plastidic invertase alters nuclear gene expression with sucrose treatment partially via GENOMES UNCOUPLED1-mediated signaling. **New Phytol** 206: 1013–1023

Meurer J, Meierhoff K, Westhoff P (1996) Isolation of high-chlorophyll-fluorescence mutants of *Arabidopsis thaliana* and their characterisation by spectroscopy, immunoblotting, and Northern hybridisation. **Planta** 198: 385–396

Morita-Yamamuro C, Tsutsui T, Tanaka A, Yamaguchi J (2004) Knock-out of the plastid ribosomal protein S21 causes impaired photosynthesis and sugar-response during germination and seedling development in *Arabidopsis thaliana*. **Plant Cell Physiol** 45: 781–788

Munoz-Nortes T, Perez-Perez JM, Ponce MR, Candela H, Micol JL (2017) The ANGULATA7 gene encodes a DnaJ-like zinc finger-domain protein involved in chloroplast function and leaf development in *Arabidopsis*. **Plant J** 89: 870–884

Murashige T, Skoog F (1962) A revised medium for rapid growth and bioassays with tobacco tissue cultures. **Physiol Plant** 15: 473–497

Neuhaus HE, Emes MJ (2000) Nonphotosynthetic metabolism in plastids. **Annu Rev Plant Physiol Plant Mol Biol** 51: 111–140

Nott A, Jung HS, Koussevitzky S, Chory J (2006) Plastid-to-nucleus retrograde signaling. **Annu Rev Plant Biol** 57: 739–759

Oliveira IC, Coruzzi GM (1999) Carbon and amino acids reciprocally modulate the expression of glutamine synthetase in *Arabidopsis*. **Plant Physiol** 121: 301–310

Peng L, Ma J, Chi W, Guo J, Zhu S, Lu Q, Lu C, Zhang L (2006) LOW PSII ACCUMULATION1 is involved in efficient assembly of photosystem II in *Arabidopsis thaliana*. **Plant Cell** 18: 955–969

Pesaresi P, Masiero S, Eubel H, Braun HP, Bhushan S, Glaser E, Salamini F, Leister D (2006) Nuclear photosynthetic gene expression is synergistically modulated by rates of protein synthesis in chloroplasts and mitochondria. **Plant Cell** 18: 970–991

Pesaresi P, Schneider A, Kleine T, Leister D (2007) Interorganellar communication. **Curr Opin Plant Biol** 10: 600–606

Pesaresi P, Varotto C, Meurer J, Jahns P, Salamini F, Leister D (2001) Knock-out of the plastid ribosomal protein L11 in *Arabidopsis*: Effects on mRNA translation and photosynthesis. **Plant J** 27: 179–189

Pogson BJ, Albrecht V (2011) Genetic dissection of chloroplast biogenesis and development: An overview. **Plant Physiol** 155: 1545–1551

Pogson BJ, Woo NS, Forster B, Small ID (2008) Plastid signalling to the nucleus and beyond. **Trends Plant Sci** 13: 602–609

Remans T, Nacry P, Pervent M, Girin T, Tillard P, Lepetit M, Gojon A (2006) A central role for the nitrate transporter NRT2.1 in the integrated morphological and physiological responses of the root system to nitrogen limitation in *Arabidopsis*. **Plant Physiol** 140: 909–921

Rogalski M, Ruf S, Bock R (2006) Tobacco plastid ribosomal protein S18 is essential for cell survival. **Nucleic Acids Res** 34: 4537–4545

Rogalski M, Schottler MA, Thiele W, Schulze WX, Bock R (2008) Rpl33, a nonessential plastid-encoded ribosomal protein in tobacco, is required under cold stress conditions. **Plant Cell** 20: 2221–2237

Romani I, Tadini L, Rossi F, Masiero S, Pribil M, Jahns P, Kater M, Leister D, Pesaresi P (2012) Versatile roles of *Arabidopsis* plastid ribosomal proteins in plant growth and development. **Plant J** 72: 922–934

Sato T, Maekawa S, Yasuda S, Sonoda Y, Katoh E, Ichikawa T, Nakazawa M, Seki M, Shinozaki K, Matsui M, Goto DB, Ikeda A, Yamaguchi J (2009) CNI1/ATL31, a RING-type ubiquitin ligase that functions in the carbon/nitrogen response for growth phase transition in *Arabidopsis* seedlings. **Plant J** 60: 852–864

Schagger H, Cramer WA, von Jagow G (1994) Analysis of molecular masses and oligomeric states of protein complexes by blue native electrophoresis and isolation of membrane protein complexes by two-dimensional native electrophoresis. **Anal Biochem** 217: 220–230

Sullivan JA, Gray JC (1999) Plastid translation is required for the expression of nuclear photosynthesis genes in the dark and in roots of the pea lip1 mutant. **Plant Cell** 11: 901–910

Suorsa M, Sirpio S, Allahverdiyeva Y, Paakkarinen V, Mamedov F, Styring S, Aro EM (2006) PsbR, a missing link in the assembly of the oxygen-evolving complex of plant photosystem II. **J Biol Chem** 281: 145–150

Tadini L, Pesaresi P, Kleine T, Rossi F, Guljamow A, Sommer F, Muhlhaus T, Schroda M, Masiero S, Pribil M, Rothbart M, Hedtke B, Grimm B, Leister D (2016) GUN1 controls accumulation of the plastid ribosomal protein S1 at the protein level and interacts with proteins involved in plastid protein homeostasis. **Plant Physiol** 170: 1817–1830

Thimm O, Blasing O, Gibon Y, Nagel A, Meyer S, Kruger P, Selbig J, Muller LA, Rhee SY, Stitt M (2004) MAPMAN: A user-driven tool to display genomics data sets onto diagrams of metabolic pathways and other biological processes. **Plant J** 37: 914–939

Tiller N, Bock R (2014) The translational apparatus of plastids and its role in plant development. **Mol Plant** 7: 1105–1120

Tiller N, Weingartner M, Thiele W, Maximova E, Schottler MA, Bock R (2012) The plastid-specific ribosomal proteins of *Arabidopsis thaliana* can be divided into non-essential proteins and genuine ribosomal proteins. **Plant J** 69: 302–316

Timmis JN, Ayliffe MA, Huang CY, Martin W (2004) Endosymbiotic gene transfer: Organelle genomes forge eukaryotic chromosomes. **Nat Rev Genet** 5: 123–135

Trapnell C, Williams BA, Pertea G, Mortazavi A, Kwan G, van Baren MJ, Salzberg SL, Wold BJ, Pachter L (2010) Transcript assembly and quantification by RNA-Seq reveals unannotated transcripts and isoform switching during cell differentiation. **Nat Biotechnol** 28: 511–515

Xiao Y, Savchenko T, Baidoo EE, Chehab WE, Hayden DM, Tolstikov V, Corwin JA, Kliebenstein DJ, Keasling JD, Dehesh K (2012) Retrograde signaling by the plastidial metabolite MEcPP regulates expression of nuclear stress-response genes. **Cell** 149: 1525–1535

Yamaguchi K, Subramanian AR (2000) The plastid ribosomal proteins. Identification of all the proteins in the 50S subunit of an organelle ribosome (chloroplast). **J Biol Chem** 275: 28466–28482

Yu HD, Yang XF, Chen ST, Wang YT, Li JK, Shen Q, Liu XL, Guo FQ (2012) Downregulation of chloroplast RPS1 negatively modulates nuclear heat-responsive expression of HsfA2 and its target genes in *Arabidopsis*. **PLoS Genet** 8: e1002669

Yuan Y, Wu H, Wang N, Li J, Zhao W, Du J, Wang D, Ling HQ (2008) FIT interacts with AtbHLH38 and AtbHLH39 in regulating iron uptake gene expression for iron homeostasis in *Arabidopsis*. **Cell Res** 18: 385–397

Zhai Z, Jung HI, Vatamaniuk OK (2009) Isolation of protoplasts from tissues of 14-day-old seedlings of *Arabidopsis thaliana*. **J Vis Exp** pii: 1149

Zhang J, Yuan H, Yang Y, Fish T, Lyi SM, Thannhauser TW, Zhang L, Li L (2016) Plastid ribosomal protein S5 is involved in photosynthesis, plant development, and cold stress tolerance in *Arabidopsis*. **J Exp Bot** 67: 2731–2744

Zhang ZW, Yuan S, Xu F, Yang H, Zhang NH, Cheng J, Lin HH (2010) The plastid hexokinase pHXK: A node of convergence for sugar and plastid signals in *Arabidopsis*. **FEBS Lett** 584: 3573–3579

Zheng ZL (2009) Carbon and nitrogen nutrient balance signaling in plants. **Plant Signal Behav** 4: 584–591

Zhuo D, Okamoto M, Vidmar JJ, Glass AD (1999) Regulation of a putative high-affinity nitrate transporter (Nrt2;1At) in roots of *Arabidopsis thaliana*. **Plant J** 17: 563–568

Zsogon A, Szakonyi D, Shi X, Byrne ME (2014) Ribosomal protein RPL27a Promotes female gametophyte development in a dose-dependent manner. **Plant Physiol** 165: 1133–1143

SUPPORTING INFORMATION

Additional Supporting Information may be found online in the supporting information tab for this article: http://onlinelibrary.wiley.com/doi/10.1111/jipb.12907/suppinfo

Figure S1. Levels of plastid transcripts in *lpe2* mutants

All mRNA transcripts were measured from wild-type and *lpe2* mutants. The graph depicts the log2 ratio of transcript levels in the mutants compared with levels in the wild-type plants. Values are means ± *SD* from three biological replicates. All transcripts of plastid genes showed minor or insignificant changes. The nitrogen response gene *NPF2.4* is used as a control.

Figure S2. The enriched cellular component terms of DEGs among wild type and *lpe2-2* mutant plants

Two additional independent biological replicates were performed, and similar results were obtained.

Figure S3. The C/N response of *lpe2* and wild type plants

(**A**) Phenotypes of *Arabidopsis* seedlings germinated and grown for 7 d on media containing different concentrations of Suc and nitrogen.100 Suc/0.1 N, 100 mM Sucrose and 0.1 mM nitrogen; 100 Suc/60N, 100 mM Sucrose and 60 mM nitrogen; 29.2 Suc/60 N, 29.2 mM Sucrose and 60 mM nitrogen;0 Suc/0.1 N, 0 mM Sucrose and 0.1 mM nitrogen; 0 Suc/60 N, 0 mM Sucrose and 60 mM nitrogen. Scale bar = 0.1 cm. 29.2 Suc/60 N medium indicate the normal concentration of C and N in 1/2 MS. Bar = 0.3 cm. (**B**) Quantification analysis of leaf areas from (**A**). Significant differences were identified at 5% (*) and 1% (**) probability levels by using Student's *t*-test.

Figure S4. The responses of *LPE2* gene expression to C/N balance

The *LPE2* mRNA transcripts were measured from the samples of Figure 6A. Values are means ± *SD* from three biological replicates. Significant differences were identified at 5% (*) and 1% (**) probability levels by using Student's *t*-test.

Table S1. A list of primers used in this study

Table S2. The differential genes of *lpe2-2*/Col-0 by transcriptome analysis